

produced a half-maximal response in satisfying this requirement. This suggests that nucleotide binding may play an important role in the *in vivo* association of nascent monomers. It also supports the conclusion that the nucleotide binding site exists in an unaltered form in the monomeric enzyme.

In contrast to the results obtained with adenine nucleotides, the experiments performed with tetrahydropteroyl triglutamate suggest that the folate binding sites are substantially altered during the dissociation process. The results of both partition equilibrium and equilibrium dialysis experiments indicate that there are four equivalent, noninteracting binding sites for tetrahydropteroyl triglutamate per mole of tetramer. This suggests that there is one folate site per monomer. However, the results obtained by both methods indicate that the monomeric enzyme does not contain an intact folate binding site. The monomer preparations had no affinity for tetrahydropteroyl triglutamate, even though greater than 80% of the monomers could still be reactivated and reassociated by incubation with NH<sub>4</sub>Cl. Such an alteration of the folate binding site is sufficient to explain why the individual monomeric subunits are catalytically inactive.

Since the dissociation and association processes are reversible, the data suggest that the folate binding sites may be formed during the association of nascent monomers to produce active formyltetrahydrofolate synthetase *in vivo*. The subunit interactions resulting from the association may cause conformational changes sufficient to produce the new binding sites. Alternatively, the folate site may be composed of segments of polypeptide chains from the two distinct subunits and is created at the site of interaction between subunits. In

either case, the tetrameric structure is essential for the formation of catalytically active formyltetrahydrofolate synthetase.

## References

- Albertsson, P.-A. (1960), *Partition of Cell Particles and Macromolecules*, New York, N. Y., Wiley.
- Curthoys, N. P., and Rabinowitz, J. C. (1971a), *J. Biol. Chem.* (in press).
- Curthoys, N. P., and Rabinowitz, J. C. (1971b), *J. Biol. Chem.*
- Curthoys, N. P., and Rabinowitz, J. C. (1971c), *J. Biol. Chem.*
- Englund, P. T., Huberman, J. A., Jovin, T. M., and Kornberg, A. (1969), *J. Biol. Chem.* 244, 3038.
- Frieden, C. (1971), *Annu. Rev. Biochem.* 40, 653.
- Gray, C. W., and Chamberlin, M. (1971), *Anal. Biochem.* 41, 83.
- Hathaway, G. M., and Crawford, I. P. (1970), *Biochemistry* 9, 1801.
- MacKenzie, R., and Rabinowitz, J. C. (1971), *J. Biol. Chem.* 246, 3731.
- Mankovitz, R., and Segal, H. L. (1969), *Biochemistry* 8, 3757.
- Rabinowitz, J. C., and Himes, R. H. (1960), *Fed. Proc., Fed. Amer. Soc. Exp. Biol.* 19, 963.
- Rabinowitz, J. C., and Pricer, W. E., Jr. (1962), *J. Biol. Chem.* 237, 2898.
- Scott, J. M., and Rabinowitz, J. C. (1967), *Biochem. Biophys. Res. Commun.* 29, 418.
- Suelter, C. H. (1970), *Science* 168, 789.
- Welch, W. H., Irwin, C. L., and Himes, R. H. (1968), *Biochem. Biophys. Res. Commun.* 30, 255.

## A Kinetic Investigation of the Crystallographically Deduced Binding Subsites of Bovine Chymotrypsin A $\gamma$ \*

David M. Segal

**ABSTRACT:** A series of seven *N*-acetyl peptide methyl ester substrates was designed and synthesized in order to probe various structural aspects of the chymotrypsin A $\gamma$  binding scheme recently proposed from crystallographic considerations by Segal, D. M., Powers, J. C., Cohen, G. H., Davies, D. R., and Wilcox, P. E. ((1971), *Biochemistry* 10, 3728). Kinetics were followed in the pH-Stat, and the *K<sub>m</sub>*'s derived from these studies were taken to be a measure of the relative binding

strengths of the substrates employed. In all cases the relative magnitudes of the observed binding energies agreed well with those predicted from the model, providing evidence that the crystallographic binding scheme is a good representation of the substrate binding mode during catalysis. The results are also more in accord with the chymotrypsin binding scheme than with an alternative scheme recently proposed for the homologous serine protease, elastase.

Recent X-ray investigations of chymotrypsin A $\gamma$  crystals treated with several peptide chloromethyl ketone inhibitors demonstrated that the resultant enzyme-inhibitor complexes involved the formation of an antiparallel  $\beta$ -type configuration between the peptide portion of the inhibitor and an extended stretch of the main chain of the enzyme (Segal *et al.*, 1971a,b).

In these studies, the enzyme-inhibitor complexes were also stabilized by the formation of a covalent link between the methylketo portion of the inhibitor and a ring nitrogen of His-57 on the enzyme. Although such a covalent bond would not be formed during catalysis, the model needed only slight alteration in order to make an ester link with Ser-195, which, according to present evidence (Cunningham, 1965) would represent the true catalytic intermediate. It was therefore proposed that the peptide binding scheme deduced from the chloromethyl ketone studies was the same as that occurring

\* From the Laboratory of Molecular Biology, National Institute of Arthritis and Metabolic Diseases, National Institutes of Health, Bethesda, Maryland 20014. Received September 23, 1971.

during enzymatic catalysis. Supporting this view was the recent discovery by Kraut and coworkers (1971) that the serine protease, subtilisin BPN', binds chloromethyl ketones in a manner almost identical with chymotrypsin, in spite of the fact that the two enzymes otherwise bear very little structural similarity to each other (Wright *et al.*, 1969; Alden *et al.*, 1970). It seemed unlikely that the resemblance of the binding-site regions was fortuitous, and that, instead, it represented an important feature of catalysis.

Nevertheless, the question of whether the inhibitor and catalytic binding modes are the same has not been fully resolved. In addition to the fact that the X-ray investigations were carried out on a noncatalytically productive complex, there also remains the suspicion that the crystallographic binding mode might reflect various artifacts arising from intermolecular interactions peculiar to the crystalline state. More perplexing were the recent X-ray studies of Shotton *et al.* (1971) on elastase-inhibitor complexes. Elastase is extremely similar to chymotrypsin, both chemically and structurally (Shotton and Watson, 1970). It was therefore disconcerting that elastase crystals were observed to bind a series of peptides at a different region from the homologue of the chloromethyl ketone binding site in chymotrypsin.

In view of these uncertainties, it was considered important to carry out experiments designed to correlate the crystallographically derived structure of the binding site with the catalytic behavior of the enzyme in solution. Toward this end, I have synthesized a number of *N*-acetyl peptide methyl ester substrates incorporating features predicted to be sensitive to various structural aspects of the proposed binding site. The esterolytic behavior of chymotrypsin A $\gamma$  toward these substrates has been examined and will be discussed in terms of the X-ray results. Related studies of the chymotrypsin-catalyzed hydrolysis of peptide substrates have also been previously described by Yoshida *et al.* (1968), by Morihara *et al.* (1969), and by Yamamoto and Izumiya (1966).

## Materials and Methods

### 1. Preparation of Substrates

**A. *N*-Acetyl-Gly-Pro-Phe-OMe.** (1) A chilled chloroform solution of 6.4 g (0.03 mole) of L-phenylalanine methyl ester·HCl (Sigma Chemical Co.), 7.5 g (0.3 mole) of Z-L-proline<sup>1</sup> (Sigma), 6.3 g (0.031 mole) of dicyclohexylcarbodiimide (DCC) (Aldrich Chemical Co.), and 4.3 ml (0.031 mole) of triethylamine was prepared and allowed to sit overnight at room temperature. The solution was filtered to remove dicyclohexylurea (DCU) and washed twice with 1 M NaHCO<sub>3</sub>, 1 M HCl, and once with H<sub>2</sub>O. The organic phase was dried over anhydrous Na<sub>2</sub>SO<sub>4</sub> and chloroform was removed by evaporation. The residue was redissolved in ethyl acetate, and additional DCU crystallized on standing. After filtration, ethyl acetate was removed by evaporation leaving 10.1 g (82% yield) of Z-Pro-Phe-OMe an oily, noncrystalline product. *Anal.* Calcd: C, 67.32; H, 6.34; N, 6.83. Found: C, 67.10; H, 6.32; N, 6.86.

(2) Z-Pro-Phe-OMe (10.1 g, 0.25 mole) was dissolved in 8 ml of glacial acetic acid and 25 ml of 33% HBr in glacial acetic acid was added. A drying tube was used to stopper the flask, and reaction was allowed to proceed for 45 min. The

product was precipitated by addition of about ten volumes of anhydrous ether, and was washed twice with ether. On addition of cyclohexane crystalline HBr-Pro-Phe-OMe was obtained. The product was filtered, washed with cyclohexane, and dried *in vacuo* over NaOH. It was then twice recrystallized by adding ether to a concentrated methanol solution of the dipeptide methyl ester. The final yield was 4.1 g (46%), and the melting range was 172.5–174.5° (uncor). *Anal.* Calcd: C, 50.43; H, 5.88; N, 7.84; Br, 22.39. Found: C, 50.45; H, 5.65; N, 7.51; Br, 22.32.

(3) A solution of 4.1 g (0.011 mole) of HBr-Pro-Phe-OMe, 1.3 g (0.011 mole) of *N*-acetylglycine (Cyclo Chemical Co.), 1.7 ml of triethylamine, and 2.3 g of DCC in chloroform was treated as in A(1). The product, *N*-Ac-Gly-Pro-Phe-OMe, crystallized from a toluene solution on addition of ice-cold petroleum ether (bp 30–60°). Filtration was carried out in the cold room, and the product was dried *in vacuo* over P<sub>2</sub>O<sub>5</sub>. *N*-Ac-Gly-Pro-Phe-OMe gave a crystalline product in the cold, or in a desiccator at room temperature, but became oily when removed from the desiccator at room temperature. The yield was 1.3 g after two further recrystallization cycles (32%). *Anal.* Calcd: C, 60.80; H, 6.67; N, 11.20. Found: C, 59.71; H, 6.88; N, 10.34.

**B. *N*-Ac-Pro-Gly-Phe-OMe.** (1) A chloroform solution of 6.3 g (0.03 mole) of Z-glycine (Sigma), 6.4 g (0.03 mole) of phenylalanine methyl ester·HCl, 6.3 g of DCC, and 4.3 ml of triethylamine was treated as in A(1). The product, Z-Gly-Phe-OMe, did not crystallize, and was obtained in a 79% yield (8.7 g). *Anal.* Calcd: C, 64.86; H, 5.95; N, 7.57. Found: C, 64.10; H, 6.08; N, 7.71.

(2) Z-Gly-Phe-OMe (8.7 g; 0.024 mole) was dissolved in 10 ml of glacial acetic acid, and 25 ml of 33% HBr in glacial acetic acid was added. Reaction was allowed to proceed for 1 hr at room temperature, and the product was precipitated by the addition of 400 ml of anhydrous ether. After washing once with ether the product crystallized. It was filtered, dried over NaOH, and recrystallized twice from methanol-ether. The yield was 5.6 g (74%) of HBr·Gly-Phe-OMe. *Anal.* Calcd: C, 45.44; H, 5.36; Br, 25.21; N, 8.84. Found: C, 44.54; H, 5.47; Br, 24.27; N, 8.86.

(3) A solution of 5.6 g (0.018 mole) of HBr·Gly-Phe-OMe, 2.8 g (0.018 mole) of *N*-Ac-L-proline (Fox Chemical Co.), 3.6 g of DCC, and 2.6 ml of triethylamine in chloroform was treated as a A(1). On addition of ethyl acetate the compound crystallized, giving 2.9 g (44% yield) of *N*-Ac-Pro-Gly-Phe-OMe. The melting range was 165.5–167.0°. *Anal.* Calcd: C, 60.80; H, 6.67; N, 11.20. Found: C, 61.00; H, 6.59; N, 11.12.

**C. *N*-Ac-Gly-Gly-Phe-OMe.** (1) *N*-Ac-glycine (5.9 g, 0.05 mole), *p*-nitrophenol (7.0 g, 0.05 mole), and DCC (10.3 g, 0.05 mole) were dissolved in chilled dimethylformamide, and reaction was allowed to proceed overnight at room temperature. DCU was removed by filtration, and the solution was concentrated by evaporation at reduced pressure. Upon addition of ether, 6.8 g of crystalline product precipitated from solution. After recrystallization from ethyl acetate-petroleum ether, 6.0 g (50% yield) of *N*-acetyl-Gly-*p*-nitrophenyl ester (Ac-Gly-ONP) was obtained: mp 117–119°. *Anal.* Calcd: C, 50.42; H, 4.20; N, 11.76. Found: C, 50.30; H, 4.42; N, 11.86.

(2) Ac-Gly-ONP (1.3 g, 0.0054 mole) and HBr·Gly-Phe-OMe (1.7 g, 0.0054 mole) were dissolved in a small volume of CHCl<sub>3</sub>, and 0.9 ml of triethylamine was added. On standing overnight at room temperature, the product formed a crystalline precipitate. The suspension was chilled and filtered, yield-

<sup>1</sup> Abbreviations used are: Z, benzyloxycarbonyl; DDC, dicyclohexylcarbodiimide; DCU, dicyclohexylurea; Ac, acetyl. Amino acids, abbreviated by the standard notation, are of the L configuration unless otherwise indicated.

ing 1.3 g of product. After recrystallization from methanol-ether 1.0 g of *N*-Ac-Gly-Gly-Phe-OMe was obtained: mp 174.5–176.5°. *Anal.* Calcd: C, 57.31; H, 6.27; N, 12.54. Found: C, 57.04; H, 6.10; N, 12.72.

*D. N-Ac-Gly-Phe-OMe.* A chilled chloroform solution of 3.0 g (0.014 mole) of *L*-phenylalanine methyl ester·HCl, 1.6 g (0.014 mole) of *N*-acetylglycine, 2.1 ml of triethylamine, and 3.0 g of DCC was treated as in A(1). On addition of water the oily residue crystallized. After filtering, the product was recrystallized from boiling water. It was observed that *N*-Ac-Gly-Phe-OMe formed a sticky, oily substance on drying, indicating that the crystalline compound was a hydrate. *Anal.* Calcd: loss on drying (*in vacuo*, overnight at 50°), 5.47% (0.89 mole of H<sub>2</sub>O/mole of *N*-Ac-Gly-Phe-OMe); C, 60.43; H, 6.47; N, 10.07. Found: C, 58.34; H, 6.73; N, 9.53. It would appear that the compound obtained was *N*-Ac-Gly-Phe-OMe·H<sub>2</sub>O, in which the water is not completely removed with the drying conditions employed.

*E. N-Ac-L-Phe-OMe.* This compound was obtained from the Cyclo Chemical Co.

*F. N-Ac-Gly-Val-Phe-OMe.* (1) A chloroform solution of 5 g (0.02 mole) of *Z*-*L*-valine (Cyclo), *L*-phenylalanine methyl ester·HCl (4.3 g, 0.02 mole), 4.2 g of DCC, and 3 ml of triethylamine was treated as in A(1). The residue was dissolved in a small amount of methanol and crystallized on addition of water. The yield was 7.0 g (86%) of *Z*-Val-Phe-OMe. *Anal.* Calcd: C, 66.33; H, 6.53; N, 7.04. Found: C, 68.96; H, 7.25; N, 7.63. The melting range was 135–137°.

(2) The carbobenzoxy group was removed from 7 g of *Z*-Val-Phe-OMe as described in A(2). On addition of ether HBr·Val-Phe-OMe gave a solid precipitate. It was recrystallized once from methanol-ether. The yield was 3.3 g (54%), and the melting range 183–187°. *Anal.* Calcd: C, 50.14; H, 6.41; Br, 22.28; N, 7.80. Found: C, 51.28; H, 6.55; Br, 23.80; N, 7.53.

(3) A chloroform solution of Ac-Gly-ONP (2.1 g, 0.009 mole), HBr·Val-Phe-OMe (3.2 g, 0.009 mole), and 1.4 ml of triethylamine was allowed to stand overnight at room temperature. A fraction of the product came out of solution on standing and ether was added to precipitate the remaining portion. After recrystallizing from boiling methanol and methanol-water, 1.8 g (54%) of Ac-Gly-Val-Phe-OMe was obtained. The melting range was 199–201°. *Anal.* Calcd: C, 60.48; H, 7.16; N, 11.14. Found: C, 60.43; H, 6.94; N, 10.84.

*G. N-Ac-Gly-D-Val-Phe-OMe.* (1) To a chilled chloroform solution of 5 g (0.02 mole) of *Z*-*D*-valine (Cyclo) and 2.8 g (0.02 mole) of *p*-nitrophenol was added 4.2 g of DCC. After sitting several hours at room temperature DCU was removed by filtration. *L*-Phenylalanine methyl ester·HCl (4.0 g) and triethylamine (3 ml) were then added and the mixture was allowed to sit overnight at room temperature, during which time 0.6 g of *Z*-*D*-Val-Phe-OMe crystallized out of solution. Only this crop was used in further synthesis. The melting range was 195–197°. *Anal.* Calcd: C, 66.33; H, 6.53; N, 7.04. Found: C, 66.40; H, 6.52; N, 6.85.

(2) *Z*-*D*-Val-Phe-OMe was suspended in 5 ml of glacial acetic acid and 10 ml of 30% HBr in glacial acetic acid was added. After sitting 1 hr in an anhydrous atmosphere several volumes of dry ether were added, and 0.45 g of HBr·*D*-Val-Phe-OMe crystallized from solution. The product was filtered, dried, and dissolved in chloroform. An equimolar amount of Ac-Gly-ONP was added along with 0.2 ml of triethylamine. After sitting overnight at room temperature, the solution was extracted one time each with 1 *N* HCl, 1 *N*

NaHCO<sub>3</sub>, and water. The organic phase was dried over anhydrous Na<sub>2</sub>SO<sub>4</sub> and the volume reduced by evaporation. On addition of ether, 150 mg of *N*-Ac-Gly-*D*-Val-Phe-OMe crystallized from solution. The melting range was 246–248°. *Anal.* Calcd: C, 60.48; H, 7.16; N, 11.14. Found: C, 60.72; H, 7.26; N, 11.05.

## II. Kinetic Measurements

Esterolysis was followed with a pH-Stat using a Radiometer TTT1 titrator and a SBR2c titrigraph. The reaction was carried out in a 20-ml water-jacketed cell at 25.0 ± 0.1°, at pH 7.00. Nitrogen was blown over the top of the reaction mixture to exclude CO<sub>2</sub>, and a Corning combination semimicro pH electrode was used to measure pH.

During esterolysis, pH was maintained constant by the addition of NaOH solutions of varying basicity. NaOH solutions were chosen so as to give readily measurable tracings for the concentrations of substrates employed, and their absolute normalities were determined by titrating standard benzoic acid solutions to neutrality under the same conditions used in the pH-Stat experiments. NaOH concentrations typically varied from 0.2 to 0.005 *N*. Corrections based on blank titrations were made at the lower base concentrations. Reaction mixtures in all experiments were degassed by boiling and contained 0.1 *M* NaCl, 5% dimethylformamide, and varying concentrations of substrate in a total volume of 10 ml.

Reactions were initiated by the addition of 50 µg of  $\gamma$ -chymotrypsin in 10<sup>-3</sup> *N* HCl. Enzyme concentrations were chosen to give a measurable hydrolysis rate under the conditions employed. The enzyme used was twice recrystallized Worthington  $\gamma$ -chymotrypsin lot CDG 6204-5 and concentrations were determined spectrophotometrically assuming  $E_{282} = 2.08$  (mg cm/ml)<sup>-1</sup> (Schwert and Kaufman, 1951).

At each substrate concentration esterolytic reactions were followed in duplicate. In many cases, the initial portions of the base uptake *vs.* time plots were linear, and rates were determined directly from their slopes. However such plots were not linear when  $K_m$  and  $[S]$  (the substrate concentrations) were of the same order of magnitude, or when  $K_m \gg [S]$ . In the former case, plots of  $1/v$  *vs.*  $1/[S]$  were found to be linear over much of the reaction and initial velocities were therefore taken from these plots at the appropriate value of  $1/[S]$ .

In the case where  $K_m \gg [S]$ , reactions were essentially first order in substrate concentration. As expected  $-\ln [S]$  *vs.* time plots were linear, and initial rates were determined from the slope and the substrate concentrations at the start of the reaction.

## Results

The chymotrypsin-catalyzed hydrolysis of a number of substrates was followed as a function of time in the pH-Stat at 25.0°, pH 7.00, and initial reaction rates were determined at various substrate concentrations, as described in the Methods section. Data were analyzed with Lineweaver-Burk and  $[S]/v$  *vs.*  $[S]$  reciprocal plots, assuming simple Michaelis-Menten kinetics, and the results are shown in Table I. Apparent catalytic constants ( $k_{cat}^{app}$ ) were derived from the least-squares slopes of the  $[S]/v$  *vs.*  $[S]$  plots. These values were then used as intercepts of Lineweaver-Burk plots, and the least-squares slopes gave  $K_m^{app}/k_{cat}^{app}$ . Standard deviations were calculated for each plot, and errors were estimated by adding 2 $\sigma$  to the lowest calculated point and subtracting 2 $\sigma$  from the highest. The new slope derived from the two points was

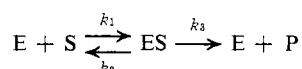
TABLE I: Apparent Kinetic Parameters for the Hydrolysis of Peptide Methyl Esters by Chymotrypsin A<sub>7</sub>.<sup>a</sup>

Peptide	$K_m^{\text{app}}$ (mM)	$k_{\text{cat}}^{\text{app}}$ (min <sup>-1</sup> ) × 10 <sup>-3</sup>
Ac-Phe	0.96 ± 0.22	1.82 ± 0.25
Ac-Gly-Phe	0.57 ± 0.15	2.53 ± 0.34
Ac-Gly-Gly-Phe	0.117 ± 0.038	3.51 ± 0.30
Ac-Pro-Gly-Phe	0.99 ± 0.29	2.24 ± 0.37
Ac-Gly-Pro-Phe	0.038 ± 0.013	1.93 ± 0.02
Ac-Gly-Val-Phe	0.021 ± 0.010	2.37 ± 0.02
Ac-Gly-D-Val-Phe	2.0 ± 1.1	0.149 ± 0.033

<sup>a</sup> Reactions were followed in 0.1 M NaCl-5% dimethyl-formamide at 25°. All optically active amino acid residues were of the L configuration except for the D-valine in the last row.

considered to represent the limit of uncertainty. Errors in  $K_m^{\text{app}}$  and  $k_{\text{cat}}^{\text{app}}$  were then derived from the estimated errors in slope, and are indicated in Table I.

In a simple Michaelis-Menten type of system where



and the  $k_3$  step is rate limiting, the derived  $K_m$  (e.g., from a Lineweaver-Burk plot) is the dissociation constant for the  $E + S \rightleftharpoons ES$  equilibrium, while  $k_{\text{cat}}$  is a direct measure of  $k_3$ . It has been known for several years however, that enzymatic catalysis in chymotrypsin follows a more complicated mechanism involving an acyl-enzyme intermediate,  $ES'$



Zerner and Bender (1964) have shown that in this type of system where the  $K_s$  equilibrium is established much more rapidly than acylation the observed Michaelis constant,  $K_m^{\text{app}}$ , is related to the true equilibrium constant,  $K_s$ , by the equation:

$$K_m^{\text{app}} = \frac{k_3}{k_2 + k_3} K_s \quad (1)$$

and that

$$k_{\text{cat}}^{\text{app}} = \frac{k_3 k_2}{k_2 + k_3} \quad (2)$$

The purpose of the present investigation is to correlate the relative strengths of binding of a series of substrates with the structure of the crystallographically derived binding site of chymotrypsin. The quantity needed for this correlation is  $K_s$ , whereas the measured quantity is  $K_m^{\text{app}}$ . Unfortunately to derive  $K_s$  from  $K_m^{\text{app}}$  the relative rates of acylation and deacylation (i.e.,  $k_2$  and  $k_3$ ) must be known and these quantities are not derivable from the present data.

It is unlikely, however, that  $k_2$  and  $k_3$  are very different for the substrates examined (except for *N*-Ac-Gly-D-Val-Phe-OMe, which will be discussed below). This presumption is based on the fact that the observed quantity,  $k_{\text{cat}}^{\text{app}}$  which is a

function only of  $k_2$  and  $k_3$  (eq 2), is similar for the first six substrates of Table I. If  $k_2$  and  $k_3$  did change to a significant degree, then they would have had to do so in such a way that the right side of eq 2 remained relatively constant. Since the rate of acylation of chymotrypsin by *N*-acetyl-L-phenylalanine methyl ester is nearly four times the deacylation rate (Zerner *et al.*, 1964), this means that, for the most part,  $k_3$  would have to be relatively constant for the first six substrates of Table I. It does not preclude large increases in the rate of acylation ( $k_2$ ), although large (by a factor of 4 or more) decreases would be detected by a drop in  $k_{\text{cat}}^{\text{app}}$ . Thus the relative constancy of  $k_{\text{cat}}^{\text{app}}$  values is consistent with, but does not unambiguously prove that  $k_3/k_2$  is nearly the same for the substrates of interest.

In fact there is no reason to expect *a priori* that  $k_2$  and  $k_3$  should vary greatly. These constants refer to the rates of acylation and deacylation of the enzyme, processes which occur in the vicinity of the bond being cleaved. They should depend primarily on the intrinsic chemical reactivity of the scissile ester or amide, and on the position which it adopts on the enzyme relative to the catalytically important residues (e.g., Ser-195 or His-57) (Henderson, 1970; Steitz *et al.*, 1969). Now in the first six substrates of Table I, the scissile bond will most likely be positioned rather precisely on the protein by a strong hydrophobic interaction with the phenyl group and by a hydrogen bond with the acylamido group of the C-terminal phenylalanine.<sup>2</sup> Differences between the various substrates occur on the acylamido portion of the scissile phenylalanine, and would be expected to affect the acylamido binding energy rather than the position of the substrate relative to the enzyme (except in the substrate involving a D-valine). Moreover since the substrates of Table I all contain  $\text{CH}_2\text{CONH-CH}(\text{CH}_2\text{C}_6\text{H}_5)\text{COOCH}_3$  moieties at their C termini, any variation between them occurs at a position widely displaced from the scissile bond. It is unlikely therefore that the intrinsic reactivities of the ester functions would differ significantly in the substrates examined.

It will therefore be assumed in subsequent discussion that  $k_2$  and  $k_3$  do not vary greatly from one substrate to another. As a result of this assumption, the  $K_m^{\text{app}}$  values listed in Table I are expected to give a good indication of the relative binding strengths of the different substrates. They differ however from the true equilibrium constants by an unknown factor involving  $k_2$  and  $k_3$  (eq 1).

## Discussion

The substrate binding scheme which is being tested in this paper is shown in Figures 1 and 2. The illustrations<sup>3</sup> represent the proposed binding mode for the peptide, *N*-Ac-Ala-Ala-Phe, covalently linked to the enzyme through an ester bond involving the side-chain oxygen of Ser-195. It is the structure proposed by Segal *et al.* (1971a,b) for the acyl-enzyme intermediate. For convenience, the notation of Schechter and Berger (1967) will be used in describing the binding site.

<sup>2</sup> This is apparently not the case with all serine proteases. Thompson and Blout (1970) have recently obtained kinetic evidence with elastase indicating that certain substrates can adopt a variety of positions on the enzyme. They explain this by the fact that in elastase the side chain of the scissile residue makes a weak interaction with the enzyme (Shotton *et al.*, 1971), thus permitting alternative binding modes. In chymotrypsin, by way of contrast, the analogous side chain is the strongly bound aromatic group.

<sup>3</sup> The illustrations have been kindly prepared by Dr. Gerson H. Cohen using the ORTEP II program of Johnson (1965, 1971).

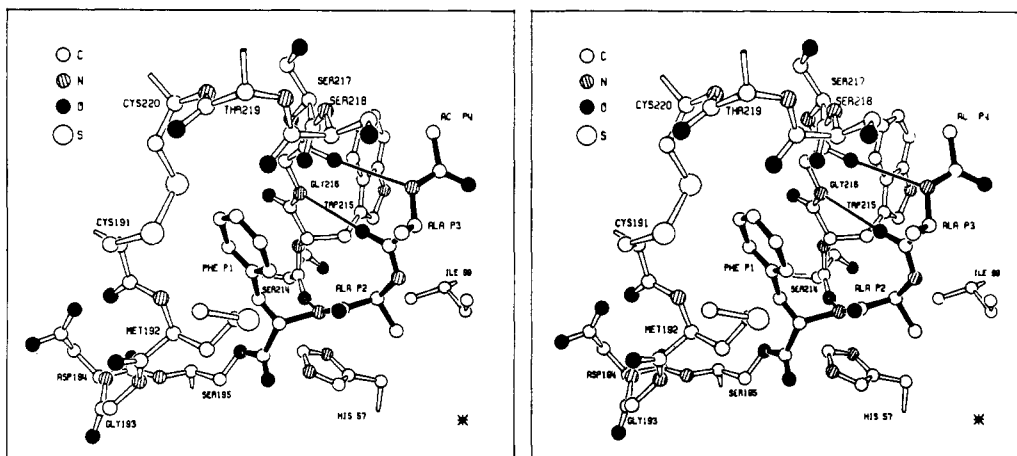


FIGURE 1: Stereo representation of the acyl-enzyme binding scheme as proposed by Segal *et al.* (1971a,b). The drawing depicts the substrate, *N*-Ac-Ala-Ala-Phe (in black), bound covalently through an ester link with the side-chain oxygen of Ser-195. Only the portion of the enzyme which may interact with the enzyme is shown.

According to this scheme, the binding site is partitioned into a series of subsites, each corresponding to a residue of the substrate. The residue on the C-terminal end of the bond being cleaved (the "scissile residue") will be termed P1, and subsequent residues in a C to N direction will be called P2, P3, and so on. That portion of the enzyme binding P1 will be called the S1 subsite, and S2, S3, etc., will refer to the binding subsites of P2, P3, etc.

The first three peptides of Table I were designed to measure the effect of substrate length on catalysis. From the model (Figures 1 and 2) we would expect that *N*-Ac-Phe-OMe would bind to the enzyme with stabilization arising mainly from the favorable aromatic side-chain interactions (Birktoft *et al.*, 1970; Steitz *et al.*, 1969; Henderson, 1970; Davies *et al.*, 1971, unpublished data) and from the formation of a hydrogen bond between the NH of the substrate and the backbone CO of Ser-214. *N*-Ac-Phe-OMe might also be stabilized by favorable interactions with S2 since the acetyl group is analogous to the  $\alpha$ -carbon and carbonyl groups of a P2 residue.

In addition to the single hydrogen bond formed by *N*-Ac-Phe-OMe, *N*-Ac-Gly-Phe-OMe can form a second hydrogen bond between the NH of Gly-216 and the CO of the acetyl group, an S3-P3 interaction. Both *N*-Ac-Phe-OMe and *N*-Ac-Gly-Phe-OMe might also be stabilized at S2 by van der Waals or hydrophobic interactions between the  $\alpha$  and carbonyl carbons of the P2 residue and the  $\beta$  carbon of Trp-215.

TABLE II: The Increase in Binding Energy ( $\Delta F_{inc}$ ) for a Given Peptide over That of *N*-Ac-Phe-OMe.<sup>a</sup>

Peptide Methyl Ester	$\Delta F_{inc}$ (kcal/mole)
Ac-Phe	0 (by definition)
Ac-Gly-Phe	-0.3
Ac-Gly-Gly-Phe	-1.2
Ac-Pro-Gly-Phe	0
Ac-Gly-Pro-Phe	-1.9
Ac-Gly-Val-Phe	-2.3

<sup>a</sup> Values of  $k_2$  and  $k_3$  are assumed constant for all substrates in the calculation.

The third peptide, *N*-Ac-Gly-Gly-Phe-OMe in addition to making all the interactions of *N*-Ac-Gly-Phe-OMe, could form third hydrogen bond between the NH of the P3 Gly and the CO of Gly-216. An examination of the model suggests that additional van der Waals or hydrophobic interactions probably do not occur to a significant degree with this peptide.

The  $K_m^{app}$  values listed in Table I for the first three substrates reflect the increase in the number of favorable interactions with chain length as expected from the model. Assuming that the relative magnitudes of acylation and deacylation rates are similar for the first six substrates of Table I, the increase in free energy of binding of any of these substrates over that of *N*-Ac-Phe-OMe ( $\Delta F_{inc}$ ) can be calculated from

$$\Delta F_{inc} = -RT \ln \frac{(K_m^{app})_{Ac-Phe-OMe}}{(K_m^{app})_{sub}}$$

where  $(K_m^{app})_{Ac-Phe-OMe}$  is the apparent  $K_m$  for *N*-Ac-Phe-OMe and  $(K_m^{app})_{sub}$  is the apparent  $K_m$  for a given substrate. Values for  $\Delta F_{inc}$  are given in Table II. The free energy for binding

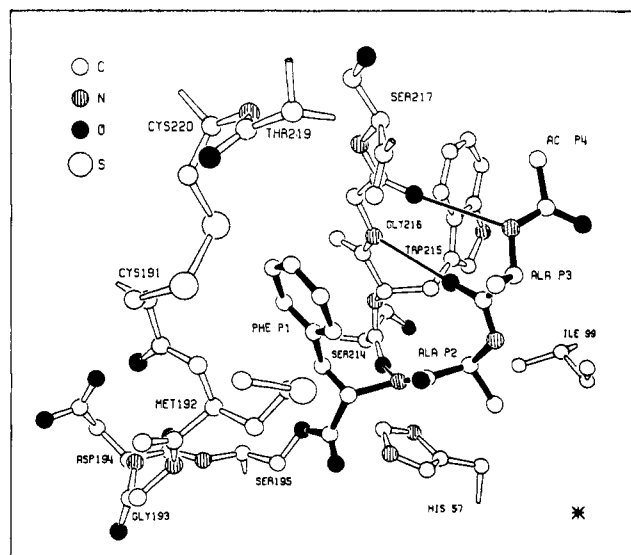


FIGURE 2: Same as Figure 1, but a single drawing.

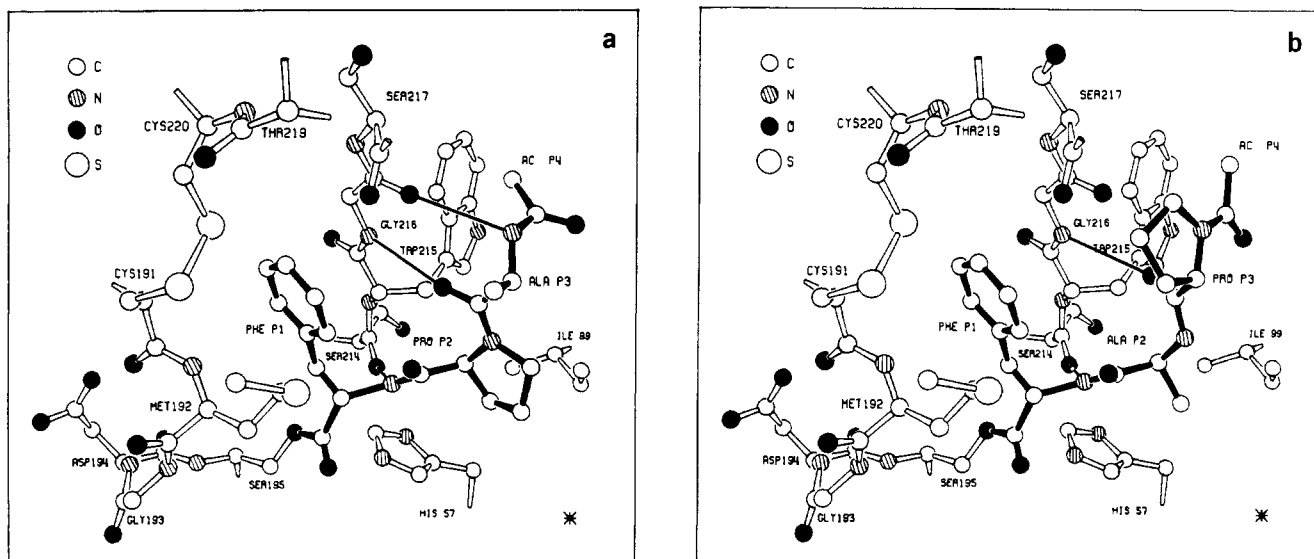


FIGURE 3: (a) Proposed enzyme-ester intermediate with a prolyl residue in P2. (b) Proposed enzyme-ester intermediate with a prolyl residue in P3.

*N*-Ac-Phe-OMe itself can be estimated from the data of Zerner *et al.* (1964) and is roughly  $-2.9$  kcal/mole. Addition of one glycyl residue decreases this by  $-0.3$  kcal/mole, while a second glycyl residue adds a further  $-0.9$  kcal/mole to the stabilization. These stabilization energies are small, and probably arise, for the most part, from the formation of the two S3-P3 hydrogen bonds.

A diagnostic feature of the model is its ability to accommodate a prolyl residue at the S2 subsite. The stereochemistry is favorable, and moreover, the fact that no hydrogen bonds are made in the S2-P2 interaction allows the tertiary amide nitrogen of the pyrrolidine ring to be substituted for the normal, unblocked peptide group without loss of hydrogen bonding. Figure 3a illustrates how a P2 proline might bind to the S2 subsite in chymotrypsin.

In contrast, a prolyl residue cannot be accommodated at the S3 subsite without loss of overall stabilization. This is a result of the loss of the hydrogen bond between the NH of P3 and the CO of Gly-216, and the unfavorable stereochemical situation arising from the pyrrolidine ring, as shown in Figure 3b. In Figure 3b the ring of the P3 proline has been drawn such that the second P3-Gly-216 hydrogen bond remains intact. In fact, this conformation appears to be sterically unacceptable due to short contacts between the P3 pyrrolidine ring and Gly-216, and it seems probable that the hydrogen bond between the P3 prolyl CO and the NH of Gly-216 would also be broken in accommodating the P3 proline.

These predictions are clearly borne out by the results of Tables I and II. Most striking is the observation that *N*-Ac-Gly-Pro-Phe-OMe is bound nearly 30-fold more tightly than *N*-Ac-Pro-Gly-Phe-OMe, corresponding to a difference of  $-1.9$  kcal/mole in binding energy. The peptide containing the P3 proline binds with just about the same energy as *N*-Ac-Phe-OMe which is the expected result if both S3-P3 hydrogen bonds were broken. A P3 prolyl residue does not appear to influence binding at S1, however, since the  $k_{cat}^{app}$  value for *N*-Ac-Pro-Gly-Phe-OMe is similar to that of *N*-Ac-Phe-OMe.

From Table I it will be observed that *N*-Ac-Gly-Pro-Phe-OMe binds to the enzyme even more strongly than *N*-Ac-Gly-Gly-Phe-OMe. This can be attributed to hydrophobic

or van der Waals interactions between the P2 pyrrolidine ring and the side chain of Ile-99 (Segal *et al.*, 1971a) or alternatively, a P2 prolyl residue might conceivably enhance binding by virtue of its restricted rotational freedom in solution. A smaller entropy decrease might thus accompany the formation of the enzyme-substrate complex. A substrate containing a P2 valyl residue, *N*-Ac-Gly-Val-Phe-OMe, was tested to help elucidate the source of the S2 stabilization forces, and it was found (Tables I and II) that this residue stabilizes the complex to even a greater degree than a P2 proline. Since the dihedral angles,  $\phi$  and  $\psi$ , of valine are expected to have a greater rotational freedom in solution than those of proline, the stronger binding of the apolar P2 valine tends to emphasize the hydrophobic nature of the S2 subsite.

In contrast to an L-valyl residue at the S2 subsite, a D-valine would be expected, from the model, to greatly hinder catalysis. Figure 4a,b show how L- and D-valyl residues might fit at S2. As indicated (4a), the side chain of the L residue points toward Ile-99, making a favorable hydrophobic interaction, while in the case of the D residue (4b), the side chain points toward the enzyme, making sterically unsatisfactory contacts with the C $\alpha$  and C $\beta$  of Trp-215. The mode of binding of a substrate containing a P2 D residue would, as a result, be drastically altered, giving rise to a change in orientation of P1, as well as P2 and P3. The movement of P1 would most likely misorient the scissile bond relative to the catalytic residues of the enzyme, leading to a decrease in both  $k_{cat}$  and binding strength. The results of Table I show this to be the case, in accord with our expectations.

Although the kinetic results of Table I are consistent with and support the view that the crystallographic and catalytic binding modes are closely related if not identical, they do not, of course, offer proof. Other binding schemes could conceivably lead to the same results. In fact, an alternative binding scheme has recently been proposed for elastase, a serine protease which is chemically and structurally homologous to chymotrypsin. From studies of elastase-inhibitor crystalline complexes, Shotton *et al.* (1971) observed that a number of peptides bind to this protease in a region different from the homolog of the chloromethyl ketone binding site of chymo-

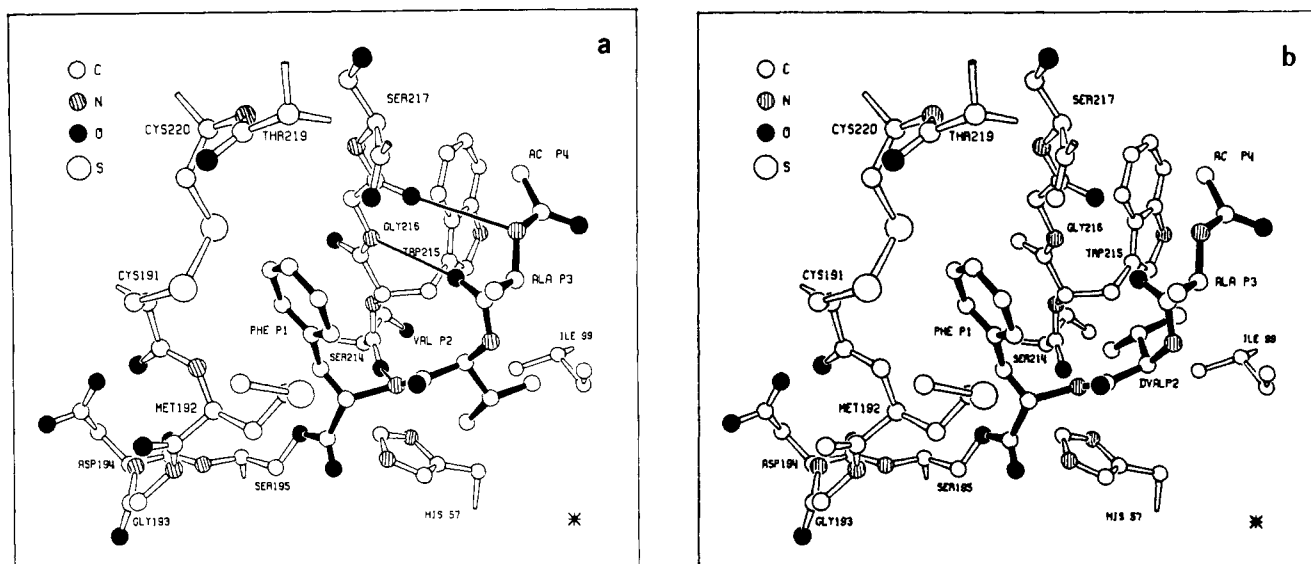


FIGURE 4: (a) Proposed enzyme-ester intermediate with a L-valyl residue at P2. (b) Proposed enzyme-ester intermediate with a D-valyl residue at P2.

trypsin. Moreover, preliminary model building studies which have recently been carried out using the chymotrypsin  $\text{A}\gamma$  model of Davies *et al.* (1971, unpublished data) suggest that at least the S1, S2, and S3 subsites of elastase have plausible analogs in chymotrypsin. The elastase model, when applied to chymotrypsin, would also predict that binding energy should increase with substrate chain length, and that a prolyl residue would fit at P2, but not P3, both of which agree with the results of the present study.

On the other hand, the elastase model would accommodate a D residue at P2 as easily as an L. Clearly this is in sharp contrast to the strict stereochemical requirement for an L residue at S2 indicated by the kinetic studies. In addition, as Shotton *et al.* (1971) point out, the elastase model would also accommodate an *N*-methyl group on P1, whereas the chloromethylketone site would not. Kinetic results which show that *N*-methyl-*N*-acetyltyrosine methyl ester is hydrolyzed with a  $k_{\text{cat}}/K_m$   $10^4$  times smaller than for *N*-acetyltyrosine methyl ester (Peterson *et al.*, 1963) again favor the view that the chloromethyl ketone binding scheme is more likely to represent the catalytic binding mode in chymotrypsin than the elastase scheme. The possibility remains, of course, that the two enzymes, elastase and chymotrypsin bind substrates differently, but this seems unlikely since both enzymes are structurally very similar at both the regions proposed as binding sites.

In conclusion, it is felt that the bulk of available evidence, including that from the present study, tends to support a binding scheme of the type illustrated in Figures 1 and 2. Although alternative binding schemes could conceivably explain the kinetic data, no binding mode has yet been observed in the crystal which would fit the kinetic results as well as that adopted by the chloromethyl ketones.

#### Acknowledgments

I thank Dr. David R. Davies of the Laboratory of Molecular Biology, National Institute of Arthritis and Metabolic Diseases, for his encouragement and useful discussions, especially with respect to the design of substrates used in this work. The aid of Dr. Gerson H. Cohen also of the same

laboratory, in the preparation of figures is also appreciated.

#### References

- Alden, R. A., Wright, C. S., and Kraut, J. (1970), *Phil. Trans. Roy. Soc. London, Ser. B* 257, 119.
- Birktoft, J. J., Blow, D. M., Henderson, R., and Steitz, T. A. (1970), *Phil. Trans. Roy. Soc. London, Ser. B* 257, 67.
- Cunningham, L. W. (1965), *Compr. Biochem.* 16, 85.
- Henderson, R. (1970), *J. Mol. Biol.* 54, 341.
- Johnson, C. K. (1965). ORTEP, ORNL-3794, Oak Ridge National Laboratory, Oak Ridge, Tenn.
- Johnson, C. K. (1971), Abstracts, American Crystallographic Association, Winter Meeting, Jan 31, Columbia, S. C., H7.
- Kraut, J., Robertus, J. D., Birktoft, J. J., and Alden, R. A. (1971), *Cold Spring Harbor Symp. Quant. Biol.* (in press).
- Morihara, K., Oka, T., and Tsuzuki, H. (1969), *Biochem. Biophys. Res. Commun.* 35, 210.
- Peterson, R. L., Hubele, K. W., and Niemann, C. (1963), *Biochemistry* 2, 942.
- Schechter, I., and Berger, A. (1967), *Biochem. Biophys. Res. Commun.* 27, 157.
- Schwert, G. W., and Kaufman, S. (1951), *J. Biol. Chem.* 190, 807.
- Segal, D. M., Cohen, G. H., Davies, D. R., Powers, J. C., and Wilcox, P. E. (1971b), *Cold Spring Harbor Symp. Quant. Biol.* (in press).
- Segal, D. M., Powers, J. C., Cohen, G. H., Davies, D. R., and Wilcox, P. E. (1971a), *Biochemistry* 10, 3728.
- Shotton, D. M., and Watson, H. C. (1970), *Nature (London)* 225, 811.
- Shotton, D. M., White, N. J., and Watson, H. C. (1971), *Cold Spring Harbor Symp. Quant. Biol.* (in press).
- Steitz, T. A., Henderson, R., and Blow, D. M. (1969), *J. Mol. Biol.* 46, 337.
- Thompson, R. C., and Blout, E. R. (1970), *Proc. Nat. Acad. Sci. U. S. A.* 67, 1734.
- Wright, C. S., Alden, R. A., and Kraut, J. (1969), *Nature (London)* 221, 235.

- Yamamoto, T., and Izumiya, N. (1966), *Arch. Biochem. Biophys.* 114, 459.  
 Yoshida, N., Yamamoto, T., and Izumiya, N. (1968), *Arch. Biochem. Biophys.* 123, 165.

- Zerner, B., and Bender, M. L. (1964), *J. Amer. Chem. Soc.* 86, 3669.  
 Zerner, B., Bond, R. P. M., and Bender, M. L. (1964), *J. Amer. Chem. Soc.* 86, 3674.

## Fast Kinetics of Adenosine Triphosphate Dependent $\text{Ca}^{2+}$ Uptake by Fragmented Sarcoplasmic Reticulum\*

Giuseppe Inesi† and Antonio Scarpa‡

**ABSTRACT:** ATP-dependent  $\text{Ca}^{2+}$  uptake by fragmented sarcoplasmic reticulum was studied by measuring light absorbancy changes undergone by murexide, a metallochromic indicator. Rapid mixing by a stopped-flow apparatus and continuous monitoring by storage oscilloscopes permitted time resolution of the initial phase.  $\text{Ca}^{2+}$  uptake proceeded linearly for the first 400–600 msec at a rate of 60–70 nmoles/mg of protein per sec (24–25°) and then declined to reach steady-state levels

in 10–15 sec. Steady-state levels, but not the initial rates, were increased by changing the ATP concentration from 0.05 to 1.25 mM. No instantaneous binding of a measurable amount of  $\text{Ca}^{2+}$  to sarcoplasmic reticulum was observed on addition of ATP. The experiments are consistent with a mechanism of active transport for the initial phase of ATP-dependent  $\text{Ca}^{2+}$  uptake by sarcoplasmic reticulum and for induction of tension decay in muscle.

Vesicular fragments of sarcoplasmic reticulum can be isolated from muscle homogenates and shown to accumulate  $\text{Ca}^{2+}$  in the presence of ATP (Hasselbach and Makinose, 1961, 1963; Ebashi and Lipmann, 1962). Measurements of the distribution of radioactive  $^{45}\text{Ca}^{2+}$  in membrane fragments and reaction mediums separated by filtration (Martonosi and Feretos, 1964), produced the following information: (a) the yield of sarcoplasmic reticulum from weight unit of muscle tissue and the maximal capacity of sarcoplasmic reticulum for  $\text{Ca}^{2+}$  accumulation *in vitro* are consistent with the amount of  $\text{Ca}^{2+}$  to be sequestered in muscle to induce relaxation; (b) the high affinity of sarcoplasmic reticulum for  $\text{Ca}^{2+}$  (Weber *et al.*, 1964, 1966) permits reduction of cytoplasmic  $\text{Ca}^{2+}$  below the concentration required for relaxation of myofibrils ( $\sim 10^{-7}$  M) (Weber *et al.*, 1963). It was therefore proposed that, *in vivo*, sarcoplasmic reticulum controls the state of contraction or relaxation of myofibrils by regulating the intracellular  $\text{Ca}^{2+}$  concentration (Hasselbach, 1964; Weber, 1966; Ebashi, 1965).

Measurements of radioactive  $^{45}\text{Ca}^{2+}$  distribution are, however, too slow to allow the determination of the initial rapid rates of  $\text{Ca}^{2+}$  uptake by sarcoplasmic reticulum. An alternative method is based on the spectrophotometric detection of changes in absorbance of the dye murexide (Ohnishi and Ebashi, 1963). This metallochromic indicator is specifically sensitive to the  $\text{Ca}^{2+}$  concentration in the medium, and its use for the measurements of  $\text{Ca}^{2+}$  transients in the presence of biological systems has been established (Mela and Chance, 1968; Jobsis and O'Connor, 1966; Geier, 1968).

Using a continuous-flow mixing device and the murexide method of detection, Ohnishi and Ebashi (1964) measured  $\text{Ca}^{2+}$  uptake by sarcoplasmic reticulum at finite times and estimated that approximately 40 nmoles of  $\text{Ca}^{2+}$  was taken up by 1 mg of sarcoplasmic reticulum within the first 30 msec of reaction. This figure, which is more than one order of magnitude higher than the initial rates of uptake extrapolated from the measurements of  $^{45}\text{Ca}^{2+}$  distribution (Weber, 1966), was attributed to ATP-induced  $\text{Ca}^{2+}$  binding to sarcoplasmic reticulum membrane (Ohnishi and Ebashi, 1964). It was proposed that this instantaneous binding is the first event in the ATP-dependent reaction of sarcoplasmic reticulum with  $\text{Ca}^{2+}$ , and the one relevant to the regulation of muscle contraction.

We have obtained continuous oscilloscopic tracings of murexide absorbancy changes in reactions initiated in a stopped flow apparatus. The rapid kinetics of  $\text{Ca}^{2+}$  uptake by sarcoplasmic reticulum were compared to the data obtained by measurements of radioactive calcium and analyzed to determine whether (a) the initial uptake occurs as instantaneous binding or displays a resolvable time dependence; (b) the initial rates of uptake may be related to those of coupled hexergonic reactions, consistent with energy-dependent ion transport; (c) an accurate quantitative relation can be established in the appropriate time scale between  $\text{Ca}^{2+}$  uptake by sarcoplasmic reticulum and its regulatory role in muscle contraction.

### Methods

Sarcoplasmic reticulum was prepared from white muscle of rabbit hind leg (McFarland and Inesi, 1971). Protein was estimated by the Folin method.

$\text{Ca}^{2+}$  uptake by sarcoplasmic reticulum was measured in reaction mixtures containing: 20 mM Tris-maleate (pH 6.8), 50 mM KCl, 10 mM  $\text{MgCl}_2$ , 140  $\mu\text{M}$  total  $\text{Ca}^{2+}$ , 100  $\mu\text{M}$  murexide (ammonium purpurate), and 0.4–1.6 mg of sarcoplasmic reticulum protein/ml. The reaction was initiated by the addi-

\* From the Johnson Research Foundation, Department of Biophysics and Physical Biochemistry, University of Pennsylvania, School of Medicine, Philadelphia, Pennsylvania 19104. Received August 30, 1971. Supported by grants from the U. S. Public Health Service (GM 12202) and from the Biomedical Kinetics Facility Evaluation, Biotechnology Resources Branch, Division of Research Resources, National Institutes of Health (71-2444).

† Permanent address: Mellon Institute, Pittsburgh, Pa. 15213.

‡ Person to whom correspondence should be addressed.